

Multi-point Conjugate Observations of Dayside ULF Waves during an Extended Period of Radial IMF

Xueling Shi¹, Michael D. Hartinger², J. B. H. Baker³, John Michael Ruohoniemi³, Dong Lin⁴, Zhonghua Xu¹, Shane Coyle³, Bharat Simha Reddy Kunduri³, Liam Kilcommons⁵, and Anna Willer⁶

¹Virginia Polytechnic Institute and State University

²Space Science Institute

³Virginia Tech

⁴National Center for Atmospheric Research

⁵University of Colorado Boulder

⁶Technical University of Denmark

November 26, 2022

Abstract

Long-lasting Pc5 ultralow frequency (ULF) waves spanning the dayside and extending from $L \sim 5.5$ into the polar cap region were observed by conjugate ground magnetometers. Observations from MMS satellites in the magnetosphere and magnetometers on the ground confirmed that the ULF waves on closed field lines were due to fundamental toroidal field line resonances (FLRs). Monochromatic waves at lower latitudes tended to maximize their power away from noon in both the morning and afternoon sectors, while more broadband waves at higher latitudes tended to have a wave power maximum near noon. The wave power distribution and anti-sunward wave propagation suggest surface waves on a Kelvin-Helmholtz (KH) unstable magnetopause coupled with FLRs. Based on satellite observations in the foreshock/magnetosheath, the more turbulent ion foreshock during an extended period of radial interplanetary magnetic field (IMF) likely plays an important role in providing seed perturbations for the growth of the KH waves.

Multi-point Conjugate Observations of Dayside ULF Waves during an Extended Period of Radial IMF

X. Shi^{1,2}, M. D. Hartinger^{3,1}, J. B. H. Baker¹, J. M. Ruohoniemi¹, D. Lin², Z. Xu¹, S. Coyle¹, B. S. R. Kunduri¹, L. M. Kilcommons⁴, and A. Willer⁵

¹Department of Electrical and Computer Engineering, Virginia Tech, Blacksburg, VA, USA.

²High Altitude Observatory, National Center for Atmospheric Research, Boulder, CO, USA.

³Space Science Institute, Boulder, CO, USA.

⁴Aerospace Engineering Sciences, University of Colorado Boulder, Boulder, Colorado, USA.

⁵National Space Institute at the Technical University of Denmark, Kgs. Lyngby, Denmark.

Key Points:

- Pc5 ULF waves were observed across the whole dayside from $L \sim 5.5$ into the polar cap region, in contrast to typical conditions
- Coordinated space and ground observations indicate that the waves on closed field lines were due to fundamental field line resonances
- The ion foreshock during radial IMF conditions provides seed perturbations for the growth of KH waves which generate the dayside ULF waves

Corresponding author: Xueling Shi, xueling7@vt.edu

Abstract

Long-lasting Pc5 ultralow frequency (ULF) waves spanning the dayside and extending from $L \sim 5.5$ into the polar cap region were observed by conjugate ground magnetometers. Observations from MMS satellites in the magnetosphere and magnetometers on the ground confirmed that the ULF waves on closed field lines were due to fundamental toroidal field line resonances (FLRs). Monochromatic waves at lower latitudes tended to maximize their power away from noon in both the morning and afternoon sectors, while more broadband waves at higher latitudes tended to have a wave power maximum near noon. The wave power distribution and anti-sunward wave propagation suggest surface waves on a Kelvin-Helmholtz (KH) unstable magnetopause coupled with FLRs. Based on satellite observations in the foreshock/magnetosheath, the more turbulent ion foreshock during an extended period of radial interplanetary magnetic field (IMF) likely plays an important role in providing seed perturbations for the growth of the KH waves.

Plain Language Summary

The Earth's magnetic field lines can oscillate at ultralow frequencies (ULF: 1 mHz - 5 Hz). These natural oscillations of closed magnetic field lines, analogous to vibrations on a stretched string, are also called geomagnetic pulsations or ULF waves. ULF waves play a key role in the transfer of energy from terrestrial space to Earth's upper atmosphere. In this study, we report a long-lasting large spatial scale ULF wave event observed by ground observatories from both hemispheres. Together with satellite measurements in space, we are able to confirm that these waves were driven by upstream turbulent structures due to the interaction between matter and electromagnetic fields emitted from the Sun and the Earth's outer atmosphere and magnetic field.

1 Introduction

Ultralow frequency (ULF; 1 mHz - 5 Hz) waves were identified as micropulsations or geomagnetic pulsations on the ground over fifty years ago (e.g. Jacobs et al., 1964). Since then, they have been recognized to play an important role in magnetospheric plasma energization/loss and energy transfer from the solar wind to Earth's magnetosphere and ionosphere (Elkington et al., 1999; Mathie & Mann, 2000; Rae et al., 2008). For example, they modulate ionospheric parameters (Pilipenko, Belakhovsky, Kozlovsky, et al., 2014), affect GPS (Karatay et al., 2010; Pilipenko, Belakhovsky, Murr, et al., 2014), and cause ionospheric heating (Crowley et al., 1985; Dessler, 1959). On the one hand, ULF waves driven by external sources from the solar wind can accelerate particles in the ring current and radiation belts through drift-bounce resonance (Zong et al., 2017). On the other hand, they can be driven by unstable particle distributions in the magnetosphere (e.g. Baddeley et al., 2005; Shi et al., 2018), and dissipate their energy to the ionosphere via Joule heating through field line resonances (FLRs) (Rae et al., 2008; Hartinger et al., 2011). When propagating to the ground, ULF waves provide a useful diagnostic probe of several magnetospheric properties (Menk et al., 1999) and can potentially drive geomagnetically induced currents (GIC) that may damage technological infrastructures (Pulkkinen & Kataoka, 2006; Pulkkinen et al., 2017). The spatial variation of the frequency and amplitude of geomagnetic perturbations is particularly important for predicting GIC and radiation belt dynamics and for remote sensing magnetospheric parameters.

The excitation of toroidal Pc5 waves is mainly due to external sources, i.e., an energy source in the solar wind, magnetosheath, or magnetopause/boundary layer. Coherent oscillations in solar wind parameters can penetrate and directly drive ULF waves inside the magnetosphere (Kepko & Spence, 2003). ULF waves can also be generated by buffeting of the magnetosphere in response to solar wind pressure perturbations, such as positive or negative dynamic pressure pulses (X. Y. Zhang et al., 2010). Surface waves that are unstable to the Kelvin-Helmholtz (KH) instability on the flanks of the magne-

67 toshere are another external source for ULF wave generation (Miura, 1992). Surface
 68 waves can set up global waveguide modes and both surface waves and waveguide modes
 69 can couple to standing shear Alfvén waves through mode conversion (Rae et al., 2005).
 70 These shear Alfvén waves are often referred to as field line resonances (FLRs). In this
 71 study, we will not differentiate between resonant and non-resonant mode conversion.

72 Upstream waves originating from the ion foreshock have long been thought to drive
 73 dayside Pc3-4 pulsations (Takahashi et al., 1984; Yumoto et al., 1985), which is favored
 74 under predominately radial interplanetary magnetic field (IMF) or low cone angle con-
 75 ditions (Russell et al., 1983; Bier et al., 2014). More recent observations have shown that
 76 foreshock disturbances, such as hot flow anomalies, can also drive compressional Pc5 waves
 77 and FLRs in the dayside magnetosphere and ionosphere with significant amplitude (Hartering
 78 et al., 2013; Shen et al., 2018; Wang et al., 2018). Hybrid simulations have also shown
 79 that high-speed jets and low frequency waves can form downstream of the quasi-parallel
 80 shock in the magnetosheath (Omidi et al., 2014; Palmroth et al., 2015, 2018); these fore-
 81 shock associated disturbances and ULF waves can act as seed fluctuations for the gener-
 82 ation of KH waves on the magnetopause (Miura, 1992).

83 In this letter, we report long-lasting Pc5 waves with an unusually large spatial ext-
 84 ent (from $L \sim 5.5$ to the polar cap region on the dayside) observed by conjugate ground
 85 magnetometers during an extended period of radial IMF condition on Jan 25, 2016; on
 86 closed field lines, these correspond to the fundamental toroidal mode. We argue that these
 87 waves are due to magnetopause surface waves caused by a KH-unstable magnetopause
 88 seeded by foreshock transients.

89 2 Observations

90 2.1 Event Overview

91 Figure 1 provides an overview of the interplanetary and geomagnetic conditions dur-
 92 ing the event and maps showing locations of ground magnetometers and footprints of
 93 other measurements from satellites. The interplanetary parameters (Figure 1a-c) are ob-
 94 tained from the WIND satellite, time shifted by 45 minutes. As shown in Figure 1a-b,
 95 the IMF is dominated by the B_x component (red curve) which leads to a low cone an-
 96 gle condition and very quiet geomagnetic activity throughout the day (Figure 1d). No
 97 obvious periodic or abrupt perturbations were observed in the solar wind velocity or dy-
 98 namic pressure (Figure 1c). However, large spatial-scale long-lasting ULF waves were
 99 observed by two conjugate latitudinal ground magnetometer chains (Figure 1e). Black
 100 traces indicate measurements from geomagnetic stations along the west coast of Green-
 101 land operated by the Technical University of Denmark (DTU). Red traces indicate mea-
 102 surements from the Autonomous Adaptive Low Power Instrument Platform (AAL-PIP)
 103 ground magnetometer chain located on the 40° magnetic meridian between the 80° - 85°
 104 South geographic latitude, 70° - 79° magnetic latitude (Clauer et al., 2014). Note that the
 105 time resolution from both ground magnetometer chains is 1 s except for the ATU sta-
 106 tion which is 10 s. (There were data quality issues with the ATU station on this date,
 107 so we only show its time series in Figure 1e and exclude it from further analysis in the
 108 following sections.)

109 The auroral image obtained from the Special Sensor Ultraviolet Spectrographic Im-
 110 ager (SSUSI) on board the Defense Meteorological Satellite Program (DMSP) satellite
 111 shows that ULF waves were observed on both closed and open magnetic field lines (Fig-
 112 ure 1f). Black (red) stars indicate locations of the DTU (AAL-PIP) stations. The AAL-
 113 PIP stations (PG1-5) were mapped from the southern hemisphere using the T96 exter-
 114 nal model and IGRF08 internal model. PG0 appears to be on T96 open field lines and
 115 so cannot be mapped to the northern hemisphere. SSJ measurements from DMSP (Fig-
 116 ure S1) also indicate that THL was in the polar cap region and that soft electron pre-

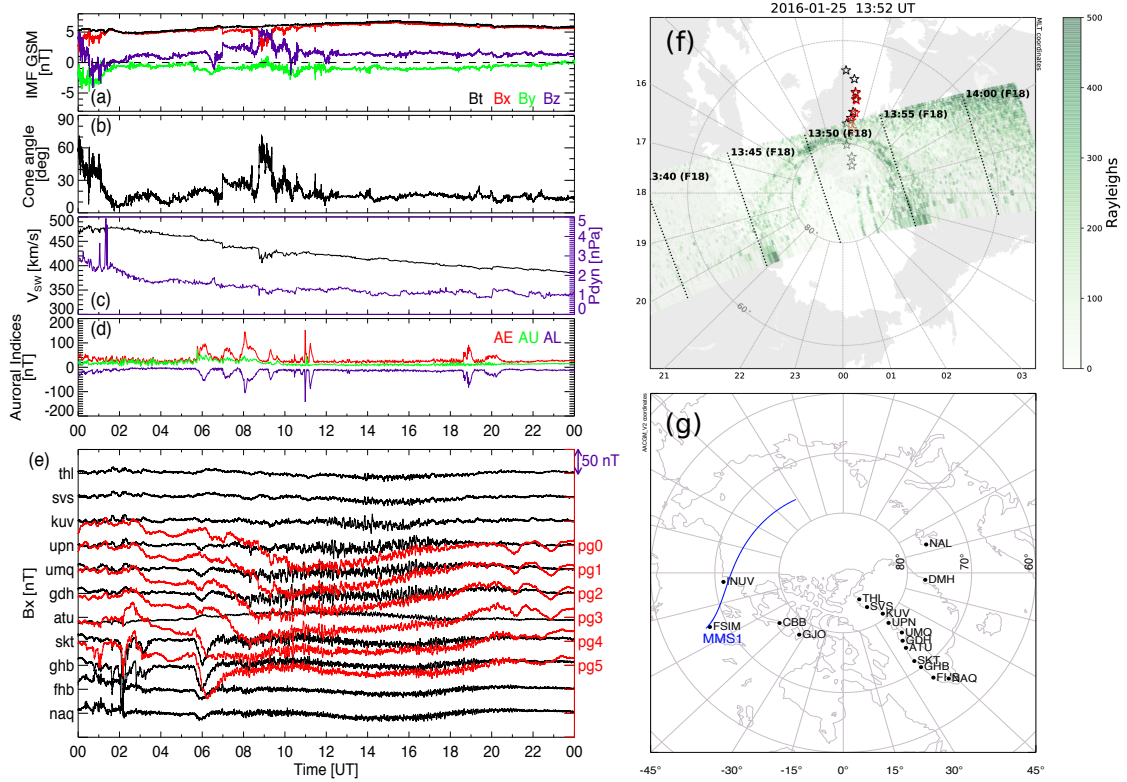


Figure 1. Event overview: (a) IMF components in GSM coordinates; (b) IMF cone angle; (c) solar wind velocity (black) and dynamic pressure (purple); (d) auroral indices; (e) time series of northward magnetic field component (B_x) in conjugate ground magnetometer observations from the DTU (black lines) stations in the northern hemisphere and the AAL-PIP (red lines) stations in the southern hemisphere; maps showing (f) DMSP SSUSI image (green pixels), locations of the DTU (black star) and AAL-PIP (red star, mapped from the southern hemisphere using the T96 external model and IGRF08 internal model) stations in magnetic local time coordinates and (g) footprint of MMS1 (blue curve) from 15 to 23 UT on Jan 25, 2016 and selected ground magnetometer locations (black dot) in AACGM coordinates.

117 cipitation was observed above it (Kilcommons et al., 2017). Figure 1g shows footprints
 118 of the MMS1 satellite from 15 to 23 UT on Jan, 25, 2016 and the locations of ground
 119 magnetometers in the northern hemisphere, including one latitudinal chain (DTU) and
 120 one longitudinal chain from which data will be analyzed in section 2.2 (Figure 2) and
 121 the FSIM and INUV stations from which data will be analyzed in section 2.3 (Figure
 122 4).

123 On the same day, long-lasting second harmonic poloidal Pc4 waves were observed
 124 in the dayside magnetosphere and ionosphere by two GOES satellites and three Super-
 125 DARN radars located at high latitudes (Shi et al., 2018). As these waves had high- m num-
 126 bers, they were screened by the ionosphere and thus not observed by the ground mag-
 127 netometers.

128 2.2 Observations from the Ground

129 In this section we present wave properties from ground magnetometer observations
 130 in both hemispheres. Figure 2 shows dynamic power spectra of magnetic field data from
 131 the two latitudinal (upper panels) and longitudinal (lower panels) chains in the north-
 132 ern hemisphere. The spectra were obtained by applying a 60 min running Fast Fourier
 133 Transform (FFT) and incrementing by 15 min so that the evolution of the wave power
 134 can be obtained. Prior to taking the FFT, the data were detrended by subtracting a 30
 135 min running average and a Hanning window was applied to reduce spectral leakage.

136 The panels in Figure 2a-b show the wave spectral power variation with latitude from
 137 the DTU chain. Noon is denoted by the second vertical line. Pc5 pulsations were mainly
 138 observed on the dayside with wave peak power frequency (black solid curve) slightly in-
 139 creasing with decreasing latitude (from top to bottom). It can be seen that the frequency
 140 stays fairly constant at all local times on the dayside. Wave power from lower latitudes
 141 (more monochromatic waves) tends to maximize away from noon in the morning/afternoon
 142 sector, while wave power from higher latitudes (more broadband waves) tends to max-
 143 imize near noon. Comparing Figure 2a (B_x) with Figure 2b (B_y) reveals wave power in
 144 the morning sector is generally greater in the B_x component (toroidal mode, Figure 2a)
 145 than in the B_y component (poloidal mode, Figure 2b). However, the wave power is com-
 146 parable for both components in the afternoon sector.

147 The panels in Figure 2c-d show the wave spectral power variation with local time
 148 from the longitudinal chain (see Figure 1g for locations). It can be clearly seen that ULF
 149 wave activity persisted across the whole dayside throughout the entire day. Five ground
 150 magnetometers located at similar magnetic latitudes but different magnetic longitudes
 151 started to pick up ULF wave activity around dawn (first vertical line on the left of the
 152 local noon annotation). The wave activity persisted toward local noon (vertical line in-
 153 dicated by the local noon annotation) and gradually disappeared in the late afternoon
 154 or dusk (vertical line on the right of the local noon annotation).

155 In Figure 3, we show time series and integrated wave power distribution for the Pc5
 156 frequency range (1-7 mHz) from two conjugate chains, i.e., the DTU chain and the AAL-
 157 PIP chain. From the inter-hemispheric comparison of magnetic field time series (see Fig-
 158 ure S2 for zoomed version), we can see that the H (B_x) component is mostly in phase
 159 between the hemispheres (Figure S2a) while the D (B_y) component is out of phase at
 160 the conjugate points (Figure S2b), which is consistent with odd mode FLR theory. The
 161 integrated wave power of the H component (Figure 3c) from higher (lower) latitudes tends
 162 to maximize (minimize) near noon. For the Pc5 toroidal component, the integrated wave
 163 power is generally stronger in the northern hemisphere (Figure 3c) than it is in the south-
 164 ern hemisphere (Figure 3e). The Pc5 wave power in the poloidal component (Figure 3d
 165 and 3f) dominates in the afternoon sector (after $\sim 14:00$ UT) and is generally stronger
 166 in the southern hemisphere.

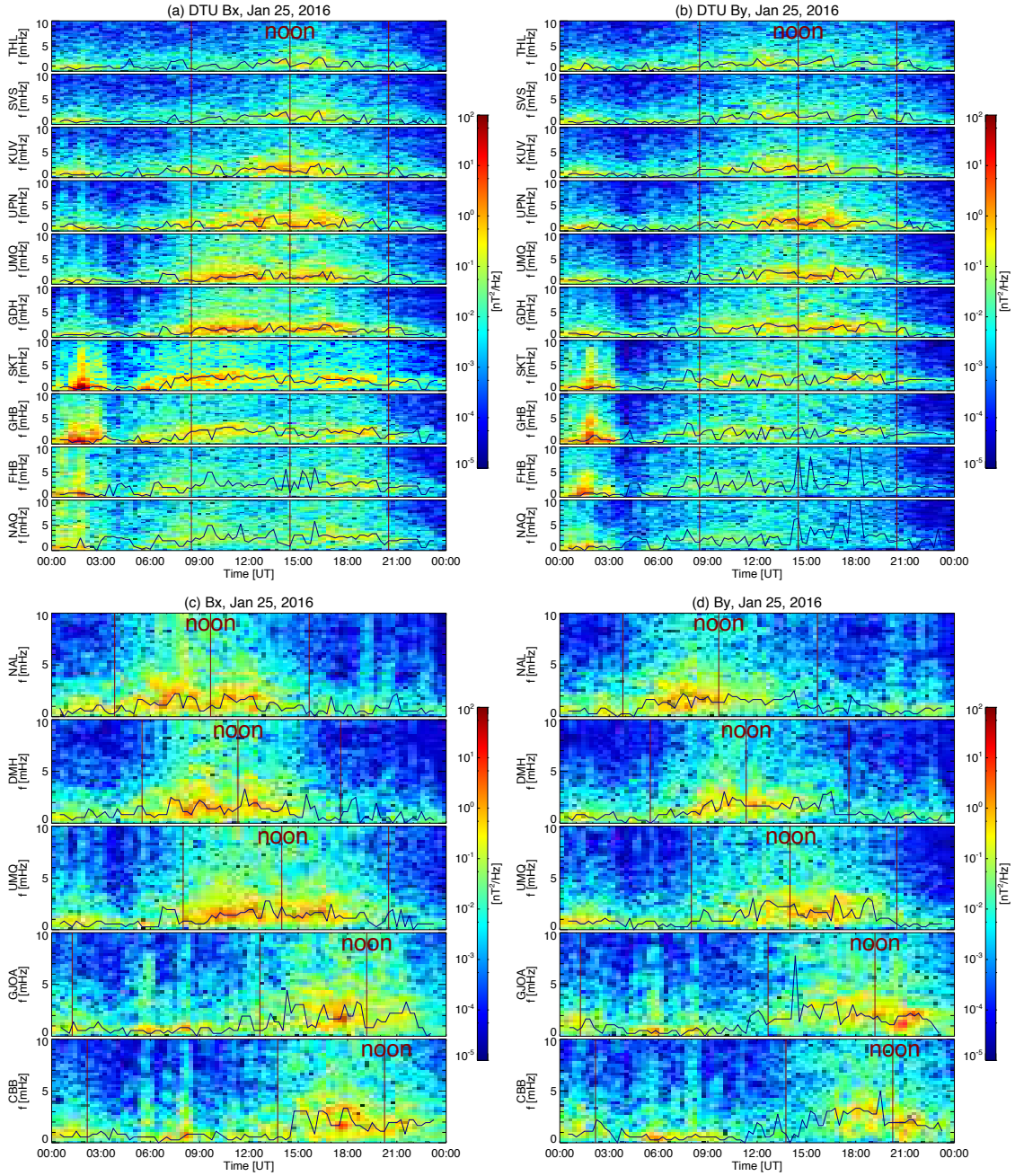


Figure 2. Dynamic power spectra of ground magnetic field (a) northward component (B_x) observed at the DTU stations; (b) eastward component (B_y) observed at the DTU stations; (c) northward component (B_x) observed at the longitudinal chain stations; (d) eastward component (B_y) observed at the longitudinal chain stations. Vertical lines indicate magnetic local times at 06 h, 12 h, and 18 h. Black solid traces identify the peak power frequency variation with time.

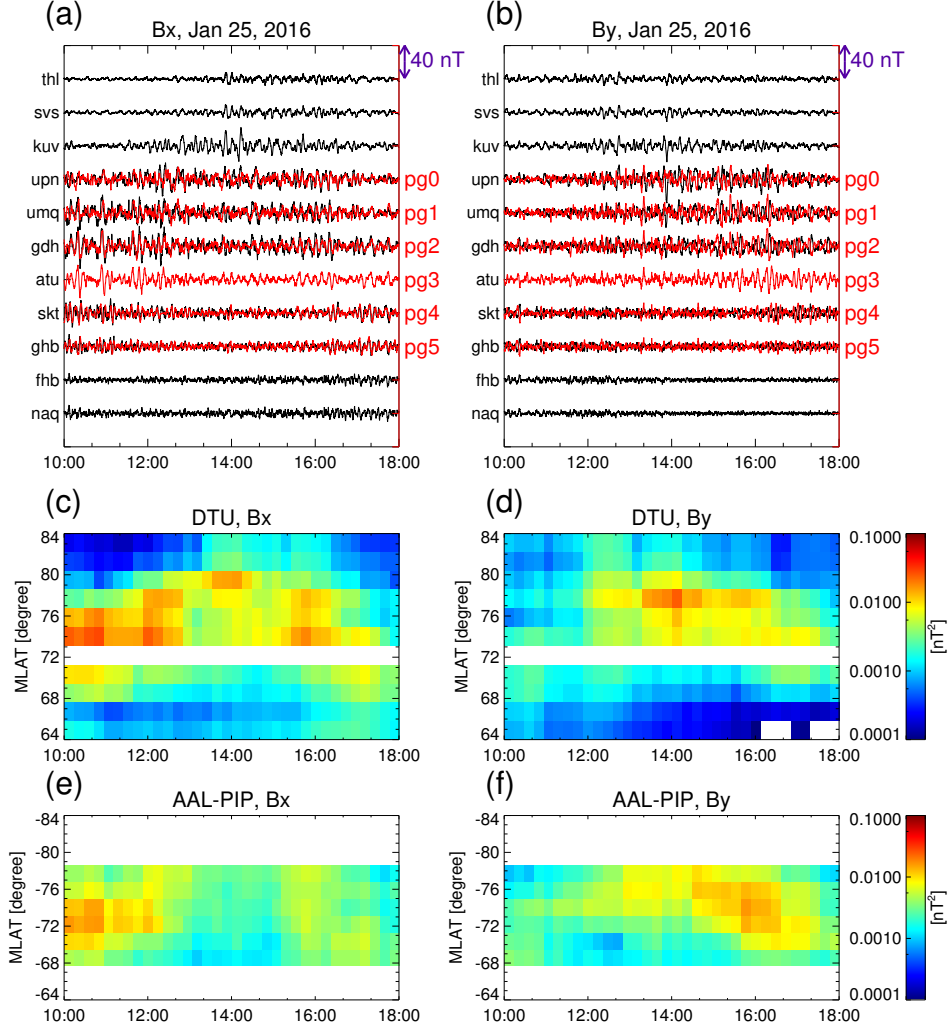


Figure 3. Inter-hemispheric comparison of ground magnetic field data from 10 to 18 UT on Jan 25, 2016 centered around local noon. Upper two panels show: (a) time series of B_x from the DTU (black) and AAL-PIP (red) stations; (b) time series of B_y from the DTU (black) and AAL-PIP (red) stations. Lower four panels show: variation of integrated wave power in the Pc5 frequency range with time and magnetic latitude for (c) DTU B_x , (d) DTU B_y , (e) AAL-PIP B_x , and (f) AAL-PIP B_y .

167 In addition to the Greenland stations, we checked the ULF wave signatures from
 168 lower L shells in the AUTUMNX stations (Connors et al., 2016) to see how far these waves
 169 can penetrate into the inner magnetosphere. Figure S3 shows that the Pc5 wave power
 170 becomes significantly weaker beyond the KJPK station ($L \sim 5.5$) and the wave power peaks
 171 at higher frequencies in the Pc3-4 frequency range at lower L shells (e.g., the VLDR sta-
 172 tion and others not shown). In addition to the ground magnetometers, the ground-based
 173 SuperDARN radars observed Pc5 ULF waves at other local times (Figure S4). As shown
 174 in Figure S4 (left) from the Inuvik radar, the waves extended deep into the polar cap.
 175 To summarize, ground magnetometers and SuperDARN radars indicate that Pc5 wave
 176 activity extended from $L \sim 5.5$ deep into the polar cap.

177 2.3 Observations from Space

178 We now analyze wave signatures in the magnetosphere from MMS satellite obser-
 179 vations. Although the observation times of the MMS satellites were different from the
 180 DTU/AAL-PIP conjugate ground magnetometer observations, the solar wind conditions
 181 were similar during this interval and the footprint of the MMS1 satellite passed near two
 182 other ground magnetometer stations (FSIM and INUV) as shown in Figure 1g. Note that
 183 MMS1 crossed the magnetopause and moved into the magnetosheath at the end of this
 184 day. Figure 4a-b shows the IMF and dynamic pressure time series from the WIND satel-
 185 lite (45 minutes shifted) indicating upstream conditions. Monochromatic Pc5 waves were
 186 observed in the B_y component (the azimuthal component in the mean-field-aligned co-
 187 ordinates) measured by MMS1 at 17-19 UT (Figure 4c-d). Wave peak power frequency
 188 (black line in Figure 4d) and wave power gradually decreased as MMS1 moved outward
 189 to higher L shells. The waveform also becomes more irregular, similar to the DTU chain
 190 observations (Figure 2a and 3a). The other three MMS satellites observed similar wave
 191 activity (not shown). FSIM and INUV stations at fixed L shells observed Pc5 waves at
 192 similar frequencies throughout the 15-23 UT time interval. Wave power and peak power
 193 frequency gradually decreased after 21 UT as these stations moved towards local noon.

194 3 Discussion

195 ULF waves extending from $L \sim 5.5$ into the polar cap region and across the whole
 196 dayside were observed by multiple ground magnetometers in both hemispheres on Jan
 197 25, 2016. Perturbations in the toroidal component generally have larger power in the north-
 198 ern hemisphere than those in the southern hemisphere (Figure 3c and 3e). The toroidal
 199 component has stronger wave power in the morning sector compared to the afternoon
 200 sector (Figures 2a, 2c, 3c and 3e). For perturbations in the poloidal component, larger
 201 amplitudes were observed in the southern hemisphere afternoon sector (Figure 3d and
 202 3f). It is unlikely that ionospheric conductivity could explain the north-south asymme-
 203 tries seen at all magnetometer station pairs since the asymmetries in precipitation and
 204 solar radiation are different at different latitudes yet we see similar patterns at all sta-
 205 tion pairs.

206 These inter-hemispheric and dawn-dusk asymmetries can be interpreted in terms
 207 of the IMF conditions and possible driving sources. As shown in Figure 1a, the IMF was
 208 dominated by an extended period of positive B_x , with slightly positive B_z and negative
 209 B_y . Stronger toroidal mode wave power in the northern hemisphere can be explained
 210 by this IMF orientation. Namely, the radially IMF dominant configuration favors for-
 211 mation of an ion foreshock upstream of the magnetopause (Eastwood et al., 2005). When
 212 both B_x and B_z are positive, a quasi-parallel foreshock favors the northern hemisphere,
 213 leading to a more turbulent magnetosheath and elevated ULF disturbances in the north-
 214 ern hemisphere (Guglielmi et al., 2017; Hwang & Sibeck, 2016).

215 The dawn-dusk asymmetry of toroidal mode standing Alfvén waves has long been
 216 attributed to the dawn-dusk asymmetry of the Kelvin-Helmholtz instability, which is ex-

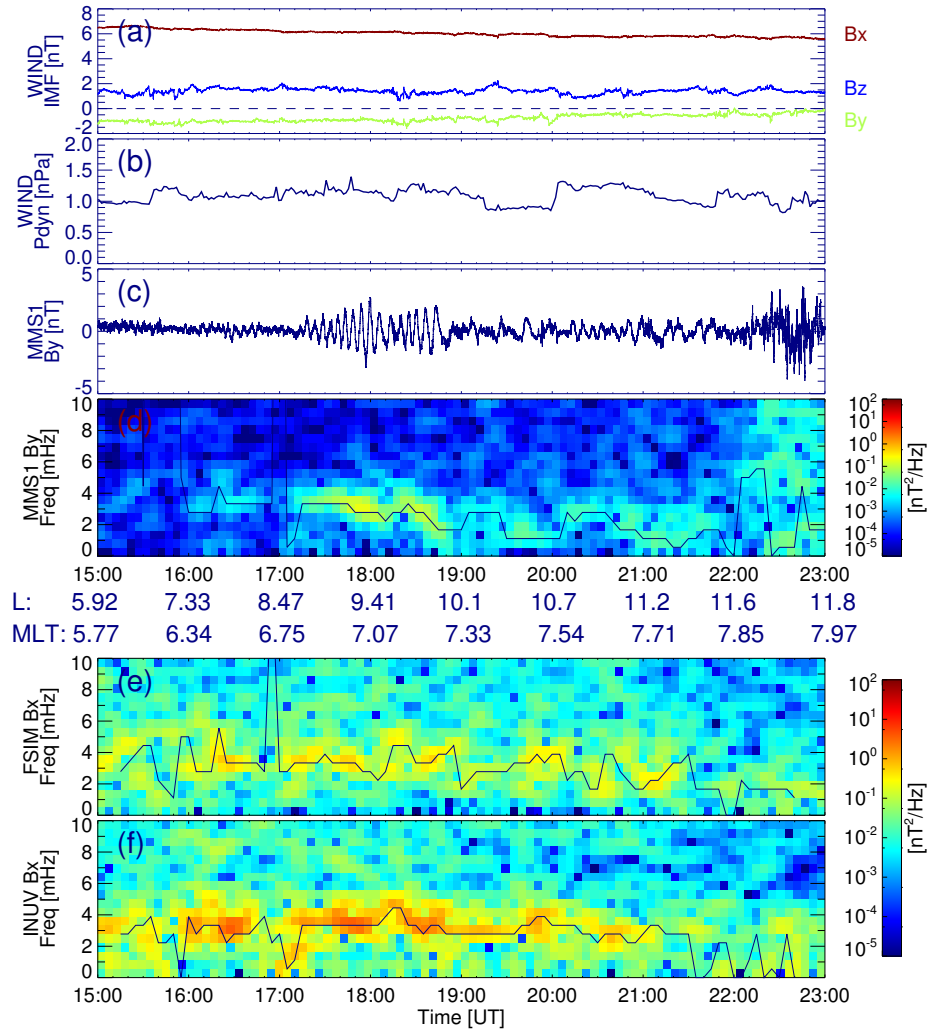


Figure 4. Coordinated observations of Pc5 waves from MMS1 and the FSIM and INUV ground magnetometers: (a) IMF components, (b) solar wind dynamic pressure, (c) MMS1 B_y time series, (d) MMS1 B_y dynamic power spectrum, (e) FSIM B_x dynamic power spectrum, and (f) INUV B_x dynamic power spectrum. Black solid traces in dynamic power spectra identify the peak power frequency variation with time.

217 pected from the asymmetry of the magnetosheath magnetic field that results from the
 218 IMF following the Parker spiral (Lee & Olson, 1980). At the same time, larger seed per-
 219 turbations for the KH-instability would be expected at dawn during spiral IMF condi-
 220 tions that favor the formation of the ion foreshock pre-noon, further enhancing surface
 221 wave amplitudes at dawn. However, Takahashi et al. (2016) have shown that fundamen-
 222 tal toroidal-mode standing Alfvén waves are stronger on the dawnside than on the dusk-
 223 side regardless of the orientation of the IMF due to the dawn-dusk asymmetry of the ra-
 224 dial profile of the mass density, and the 3D simulation work by Wright et al. (2018) also
 225 showed that FLRs are excited with larger amplitude at dawn compared to dusk in an
 226 asymmetric magnetospheric waveguide system that is driven symmetrically about the
 227 noon meridian. It is possible that both external (IMF orientation) and internal (radial
 228 mass density variation) mechanisms described above were active in the dayside magne-
 229 tosphere on Jan 25, 2016.

230 It is very unlikely that such large spatial scale and steady long-lasting ULF waves
 231 observed on the dayside were excited by instabilities internal to the magnetosphere (e.g.
 232 Shi et al., 2018), which usually excite poloidal mode waves with large azimuthal wavenum-
 233 ber that are difficult to detect with ground magnetometers (Hughes & Southwood, 1976).
 234 Thus we discuss the possibility of an external upstream source. We first exclude the so-
 235 lar wind direct driving source and solar wind pressure pulse driving source, since neither
 236 quasi-periodic solar number density/pressure or magnetic field variations at similar fre-
 237 quencies, nor large-amplitude, transient dynamic pressure pulses, were observed by the
 238 upstream WIND satellite (Figure 4a-b). One possible scenario is that the Pc5 waves ob-
 239 served on the dayside closed field lines are FLRs coupled to compressional ULF waves
 240 driven by surface waves at the KH-unstable magnetopause. We provide additional ev-
 241 idence for such a scenario:

- 242 1. The wave power distribution has a maximum around noon at higher latitudes and
 243 maxima in the morning/afternoon sector at lower latitudes (Figures 2a and 3c).
 244 The lower latitude peaks at dawn/dusk are consistent with surface waves coupling
 245 to FLRs, while the high-latitude peaks may be consistent with more direct obser-
 246 vations of the seed perturbations for the surface waves (e.g., Guglielmi et al., 2017).
- 247 2. There is an anti-sunward wave propagation in the morning and afternoon sectors
 248 from SuperDARN radar observations (Figure S4 and text in the Supporting In-
 249 formation): azimuthal wave number (James et al., 2013) estimated from the Stokkseyri
 250 radar ($m \sim 1.5$, eastward at mlt ~ 17 hours and mlat $\sim 72.5^\circ$) and the Inuvik radar
 251 ($m \sim -1.7$, westward at mlt ~ 9 hours and mlat $\sim 79.4^\circ$). This is consistent with
 252 a surface wave driver.
- 253 3. The steady northward IMF orientation (Figure 1a) possibly provides a persistent
 254 mechanism for KH wave generation (Lin et al., 2014; Kavosi & Raeder, 2015).
- 255 4. There are surface wave signatures from MMS1 observations of magnetopause os-
 256 cillations from 03:30 to 03:45 UT (Figure S5).

257 Since radial IMF orientation dominated throughout this event, an ion foreshock
 258 formed upstream of the quasi-parallel bow shock introducing a broad range of pertur-
 259 bations such as the foreshock cavity and hot flow anomaly (Sibeck et al., 2002; H. Zhang
 260 et al., 2013). The more turbulent foreshock plays an important role in providing seed
 261 perturbations for the growth of KH waves (Miura, 1992; Nosé et al., 1995; Hwang & Sibeck,
 262 2016). We also know that foreshock transients can drive magnetopause perturbations
 263 and ripples with corresponding ULF perturbations in the absence of a KH unstable mag-
 264 netopause (Sibeck, 1990). The local time distribution with peak near noon at high lat-
 265 itudes is consistent with large foreshock disturbances seeding the growth of surface waves
 266 via KHI, but it would not be consistent with the classic KHI picture where small upstream
 267 seed perturbations drive the surface waves - in this case, there is almost no wave power
 268 at noon (e.g. Claudepierre et al., 2009, 2016).

269 An outstanding issue is how Pc5 waves are generated in the cusp and polar cap re-
 270 gion on open field lines. The polar cap has generally been thought to be a quiet region,
 271 with wave power entering only from neighboring regions, such as the auroral oval (e.g.
 272 Bland & McDonald, 2016). As summarized in Engebretson et al. (2006) Pc5 waves from
 273 very high latitudes can be categorized into three classes according to their potential sources:
 274 cusp-related waves (Posch et al., 1999), polar pulsations extended from the auroral re-
 275 gion, and Pi_{cap3} independent of cusp and auroral pulsations (Yagova et al., 2004). For
 276 this particular event, it is possible the Pc5 waves on open field lines came directly from
 277 the magnetosheath and foreshock region, generating waves with very similar properties
 278 across a wide range of L, from deep in the polar cap to $L \sim 5.5$. Global ULF wave mod-
 279 els taking into account kinetic processes in the foreshock region and magnetosheath are
 280 needed to reveal the exact driving mechanism of this new type of Pc5 event extending
 281 from $L \sim 5.5$ into the polar cap.

282 Finally, it should be emphasized that the waves observed in this study can poten-
 283 tially cause geospace impacts. This study shows that during radial IMF, foreshock tran-
 284 sients/KHI can lead to the generation of spatially extended Pc5 wave activity. More work
 285 is needed to understand whether these types of waves have sufficient amplitude to gener-
 286 ate significant dB/dt and GIC. Additionally, the multi-point conjugate observations
 287 in this study reveal that during radial IMF conditions, the properties of Pc5 ULF waves
 288 - frequency and amplitude - may vary little across a wide range of latitudes, in contrast
 289 to general expectations for standing Alfvén waves driven by external energy sources; this
 290 could have implications for predicting GIC (Pulkkinen et al., 2017) and radiation belt
 291 dynamics (Elkington, 2006).

292 4 Conclusions

293 Using conjugate inter-hemispheric observations we have examined the properties
 294 of ULF waves observed across the entire dayside during an extended period of radial IMF.
 295 The waves were observed from $L \sim 5.5$ to the cusp and polar cap region with minimal
 296 frequency variations (1-4 mHz) over local time and latitude. Observations from MMS
 297 satellites and multiple inter-hemispheric ground magnetometers indicate that the Pc5
 298 pulsations on closed field lines are fundamental toroidal mode FLRs. Wave power from
 299 lower latitudes (more monochromatic waves) tends to maximize away from noon in the
 300 morning/afternoon sector, while wave power from higher latitudes (more broadband waves)
 301 tends to maximize near noon. The wave power distribution and anti-sunward propaga-
 302 tion suggest KH instability driven waves coupled with FLRs. The upstream ion foreshock
 303 may provide seed perturbations for the growth of the KH instability which generates the
 304 dayside Pc5 waves. No previous study has shown that global and steady Pc5 wave ac-
 305 tivity as reported in our study could be associated with B_x predominant conditions (or
 306 ion foreshock processes). This event is a good example of how low cone angle (and po-
 307 tentially ion foreshock processes) can be associated with Pc5 waves rather than only with
 308 Pc3-4 waves. Further investigations of this type of global and steady wave activity is needed
 309 to determine how often these driving conditions occur, to better assess how upstream
 310 foreshock/magnetosheath disturbances couple to magnetospheric ULF waves, and to de-
 311 termine whether these long-lasting Pc5 waves could cause geospace impacts such as GICs
 312 or radiation belt interactions.

313 Acknowledgments

314 The authors are grateful to Mary Hudson, Kazue Takahashi, Hui Zhang and Heli Hietala
 315 for helpful discussions and valuable comments. Work at Virginia Tech has been supported
 316 by National Aeronautics and Space Administration (NASA) Headquarters under the NASA
 317 Earth and Space Science Fellowship Program - Grant 80NSSC17K0456 P00001, National
 318 Science Foundation (NSF) grant AGS-1341918, and NASA 80NSSC19K0907. MDH, ZX,
 319 and SC were supported by NSF PLR-1543364 and PLR-1744828. DL was supported by

320 the Advanced Study Program Postdoctoral Fellowship of the National Center for Atmo-
 321 spheric Research (NCAR). NCAR is sponsored by the NSF. We acknowledge the use of
 322 DTU, AAL-PIP, and AUTUMNX ground magnetometer data. DTU data are obtained
 323 from the public Tromso Geophysical Observatory website (<http://flux.phys.uit.no/geomag.html>).
 324 The Antarctic AAL-PIP data have been provided by Virginia Tech which is supported
 325 by NSF through the following awards for this purpose: ANT0839858, ATM922979, ANT0838861,
 326 PLR-1243398, and PLR-1543364. AUTUMN/AUTUMNX groundbased magnetometer
 327 data are available at <http://autumn.athabasca.ca/> website. We also wish to acknowl-
 328 edge the use of data from the MMS and WIND spacecraft. MMS data are available via
 329 MMS science data center (at <https://lasp.colorado.edu/mms/sdc/public/>). Solar wind
 330 data from the Wind spacecraft were obtained through the CDAWeb <https://cdaweb.gsfc.nasa.gov/index.html/>.
 331 We would like to thank Johns Hopkins University Applied Physics Laboratory for pro-
 332 viding the DMSP/SSUSI auroral FUV data (available at https://ssusi.jhuapl.edu/data_products)
 333 and DMSP/SSJ data (available at <https://www.ngdc.noaa.gov/stp/satellite/dmsp/>). We
 334 also thank all participants in the worldwide SuperDARN collaboration for the distribu-
 335 tion of SuperDARN data via the website (<http://vt.superdarn.org/tiki-index.php?page=Data+Access>).

336 References

- 337 Baddeley, L., Yeoman, T., Wright, D., Trattner, K., & Kellet, B. (2005). On the
 338 coupling between unstable magnetospheric particle populations and resonant
 339 high m ULF wave signatures in the ionosphere. *ANNALES GEOPHYSICAE*,
 340 *23*(2), 567-577. doi: {10.5194/angeo-23-567-2005}
- 341 Bier, E. A., Owusu, N., Engebretson, M. J., Posch, J. L., Lessard, M. R., &
 342 Pilipenko, V. A. (2014). Investigating the IMF cone angle control of Pc3-4
 343 pulsations observed on the ground. *Journal of Geophysical Research: Space*
 344 *Physics*, *119*(3), 1797-1813. Retrieved from [https://agupubs.onlinelibrary](https://agupubs.onlinelibrary.wiley.com/doi/abs/10.1002/2013JA019637)
 345 [.wiley.com/doi/abs/10.1002/2013JA019637](https://agupubs.onlinelibrary.wiley.com/doi/abs/10.1002/2013JA019637) doi: 10.1002/2013JA019637
- 346 Bland, E. C., & McDonald, A. J. (2016). High spatial resolution radar observations
 347 of ultralow frequency waves in the southern polar cap. *Journal of Geophysical*
 348 *Research: Space Physics*, *121*(5), 4005–4016.
- 349 Claudepierre, S. G., Toffoletto, F. R., & Wiltberger, M. (2016). Global MHD
 350 modeling of resonant ULF waves: Simulations with and without a plasma-
 351 sphere. *Journal of Geophysical Research: Space Physics*, *121*(1), 227-244.
 352 Retrieved from [https://agupubs.onlinelibrary.wiley.com/doi/abs/](https://agupubs.onlinelibrary.wiley.com/doi/abs/10.1002/2015JA022048)
 353 [10.1002/2015JA022048](https://agupubs.onlinelibrary.wiley.com/doi/abs/10.1002/2015JA022048) doi: 10.1002/2015JA022048
- 354 Claudepierre, S. G., Wiltberger, M., Elkington, S. R., Lotko, W., & Hudson, M. K.
 355 (2009). Magnetospheric cavity modes driven by solar wind dynamic pressure
 356 fluctuations. *Geophysical Research Letters*, *36*(13). Retrieved from [https://](https://agupubs.onlinelibrary.wiley.com/doi/abs/10.1029/2009GL039045)
 357 agupubs.onlinelibrary.wiley.com/doi/abs/10.1029/2009GL039045 doi:
 358 [10.1029/2009GL039045](https://agupubs.onlinelibrary.wiley.com/doi/abs/10.1029/2009GL039045)
- 359 Clauer, C., Kim, H., Deshpande, K., Xu, Z., Weimer, D., Musko, S., ... others
 360 (2014). An autonomous adaptive low-power instrument platform (AAL-PIP)
 361 for remote high-latitude geospace data collection. *Geoscientific Instrumenta-*
 362 *tion, Methods and Data Systems*, *3*(2), 211.
- 363 Connors, M., Schofield, I., Reiter, K., Chi, P. J., Rowe, K. M., & Russell, C. T.
 364 (2016). The AUTUMNX magnetometer meridian chain in Québec, Canada.
 365 *Earth, Planets and Space*, *68*(1), 2.
- 366 Crowley, G., Wade, N., Waldock, J., Robinson, T., & Jones, T. (1985). High time-
 367 resolution observations of periodic frictional heating associated with a Pc5
 368 micropulsation. *Nature*, *316*(6028), 528.
- 369 Dessler, A. (1959). Upper atmosphere density variations due to hydromagnetic heat-
 370 ing. *Nature*, *184*(4682), 261.
- 371 Eastwood, J., Lucek, E., Mazelle, C., Meziane, K., Narita, Y., Pickett, J., &
 372 Treumann, R. (2005). The foreshock. *Space Science Reviews*, *118*(1-4),

- 373 41–94.
- 374 Elkington, S. R. (2006). A review of ULF interactions with radiation belt electrons.
375 *GEOPHYSICAL MONOGRAPH-AMERICAN GEOPHYSICAL UNION*, 169,
376 177.
- 377 Elkington, S. R., Hudson, M. K., & Chan, A. A. (1999). Acceleration of rela-
378 tivist electrons via drift-resonant interaction with toroidal-mode Pc-5 ULF
379 oscillations. *Geophysical Research Letters*, 26(21), 3273–3276. Retrieved
380 from [https://agupubs.onlinelibrary.wiley.com/doi/abs/10.1029/](https://agupubs.onlinelibrary.wiley.com/doi/abs/10.1029/1999GL003659)
381 1999GL003659 doi: 10.1029/1999GL003659
- 382 Engebretson, M., Posch, J., Pilipenko, V., & Chugunova, O. (2006). ULF waves at
383 very high latitudes. *Geophysical monograph*, 169, 137–156.
- 384 Guglielmi, A., Klain, B., & Potapov, A. (2017, Dec). North-south asymmetry
385 of ultra-low-frequency oscillations of Earth’s electromagnetic field. *Solar-*
386 *Terrestrial Physics*, 3(4), 26–31. doi: 10.12737/stp-34201703
- 387 Hartinger, M., Angelopoulos, V., Moldwin, M. B., Glassmeier, K.-H., & Nishimura,
388 Y. (2011). Global energy transfer during a magnetospheric field line resonance.
389 *Geophysical Research Letters*, 38(12).
- 390 Hartinger, M., Turner, D., Plaschke, F., Angelopoulos, V., & Singer, H. (2013). The
391 role of transient ion foreshock phenomena in driving Pc5 ULF wave activity.
392 *Journal of Geophysical Research: Space Physics*, 118(1), 299–312.
- 393 Hughes, W. J., & Southwood, D. J. (1976). The screening of micropulsation signals
394 by the atmosphere and ionosphere. *Journal of Geophysical Research*, 81(19),
395 3234–3240. Retrieved from [https://agupubs.onlinelibrary.wiley.com/](https://agupubs.onlinelibrary.wiley.com/doi/abs/10.1029/JA081i019p03234)
396 [doi/abs/10.1029/JA081i019p03234](https://agupubs.onlinelibrary.wiley.com/doi/abs/10.1029/JA081i019p03234) doi: 10.1029/JA081i019p03234
- 397 Hwang, K.-J., & Sibeck, D. G. (2016). Role of low-frequency boundary waves in
398 the dynamics of the dayside magnetopause and the inner magnetosphere. In
399 *Lowfrequency waves in space plasmas* (p. 213–239). American Geophysical
400 Union (AGU). Retrieved from [https://agupubs.onlinelibrary.wiley.com/](https://agupubs.onlinelibrary.wiley.com/doi/abs/10.1002/9781119055006.ch13)
401 [doi/abs/10.1002/9781119055006.ch13](https://agupubs.onlinelibrary.wiley.com/doi/abs/10.1002/9781119055006.ch13) doi: 10.1002/9781119055006.ch13
- 402 Jacobs, J. A., Kato, Y., Matsushita, S., & Troitskaya, V. A. (1964). Classification
403 of geomagnetic micropulsations. *Journal of Geophysical Research*, 69(1), 180–
404 181. Retrieved from [https://agupubs.onlinelibrary.wiley.com/doi/abs/](https://agupubs.onlinelibrary.wiley.com/doi/abs/10.1029/JZ069i001p00180)
405 [10.1029/JZ069i001p00180](https://agupubs.onlinelibrary.wiley.com/doi/abs/10.1029/JZ069i001p00180) doi: 10.1029/JZ069i001p00180
- 406 James, M. K., Yeoman, T. K., Mager, P. N., & Klimushkin, D. Y. (2013). The
407 spatio-temporal characteristics of ULF waves driven by substorm injected par-
408 ticles. *Journal of Geophysical Research: Space Physics*, 118(4), 1737–1749.
409 Retrieved from [https://agupubs.onlinelibrary.wiley.com/doi/abs/](https://agupubs.onlinelibrary.wiley.com/doi/abs/10.1002/jgra.50131)
410 [10.1002/jgra.50131](https://agupubs.onlinelibrary.wiley.com/doi/abs/10.1002/jgra.50131) doi: 10.1002/jgra.50131
- 411 Karatay, S., Arikan, F., & Arikan, O. (2010). Investigation of total electron content
412 variability due to seismic and geomagnetic disturbances in the ionosphere. *Ra-*
413 *dio Science*, 45(05), 1–12.
- 414 Kavosi, S., & Raeder, J. (2015). Ubiquity of Kelvin–Helmholtz waves at Earths mag-
415 netopause. *Nature Communications*, 6, 7019.
- 416 Kepko, L., & Spence, H. E. (2003). Observations of discrete, global magneto-
417 spheric oscillations directly driven by solar wind density variations. *Journal*
418 *of Geophysical Research: Space Physics*, 108(A6). Retrieved from [https://](https://agupubs.onlinelibrary.wiley.com/doi/abs/10.1029/2002JA009676)
419 agupubs.onlinelibrary.wiley.com/doi/abs/10.1029/2002JA009676 doi:
420 10.1029/2002JA009676
- 421 Kilcommons, L. M., Redmon, R. J., & Knipp, D. J. (2017). A new DMSP mag-
422 netometer and auroral boundary data set and estimates of field-aligned
423 currents in dynamic auroral boundary coordinates. *Journal of Geophysi-*
424 *cal Research: Space Physics*, 122(8), 9068–9079. Retrieved from [https://](https://agupubs.onlinelibrary.wiley.com/doi/abs/10.1002/2016JA023342)
425 agupubs.onlinelibrary.wiley.com/doi/abs/10.1002/2016JA023342 doi:
426 10.1002/2016JA023342
- 427 Lee, L. C., & Olson, J. V. (1980). Kelvin-helmholtz instability and the variation

- of geomagnetic pulsation activity. *Geophysical Research Letters*, 7(10), 777-780. Retrieved from <https://agupubs.onlinelibrary.wiley.com/doi/abs/10.1029/GL007i010p00777> doi: 10.1029/GL007i010p00777
- Lin, D., Wang, C., Li, W., Tang, B., Guo, X., & Peng, Z. (2014). Properties of Kelvin-Helmholtz waves at the magnetopause under northward interplanetary magnetic field: Statistical study. *Journal of Geophysical Research: Space Physics*, 119(9), 7485-7494. Retrieved from <https://agupubs.onlinelibrary.wiley.com/doi/abs/10.1002/2014JA020379> doi: 10.1002/2014JA020379
- Mathie, R. A., & Mann, I. R. (2000). A correlation between extended intervals of ULF wave power and storm-time geosynchronous relativistic electron flux enhancements. *Geophysical Research Letters*, 27(20), 3261-3264. Retrieved from <https://agupubs.onlinelibrary.wiley.com/doi/abs/10.1029/2000GL003822> doi: 10.1029/2000GL003822
- Menk, F., Orr, D., Clilverd, M., Smith, A., Waters, C., Milling, D., & Fraser, B. (1999). Monitoring spatial and temporal variations in the dayside plasmasphere using geomagnetic field line resonances. *Journal of Geophysical Research: Space Physics*, 104(A9), 19955-19969.
- Miura, A. (1992). Kelvin-Helmholtz instability at the magnetospheric boundary: Dependence on the magnetosheath sonic Mach number. *Journal of Geophysical Research: Space Physics*, 97(A7), 10655-10675. Retrieved from <https://agupubs.onlinelibrary.wiley.com/doi/abs/10.1029/92JA00791> doi: 10.1029/92JA00791
- Nosé, M., Iyemori, T., Sugiura, M., & Slavin, J. A. (1995). A strong dawn/dusk asymmetry in Pc5 pulsation occurrence observed by the DE-1 satellite. *Geophysical Research Letters*, 22(15), 2053-2056. Retrieved from <https://agupubs.onlinelibrary.wiley.com/doi/abs/10.1029/95GL01794> doi: 10.1029/95GL01794
- Omidi, N., Sibeck, D., Gutynska, O., & Trattner, K. J. (2014). Magnetosheath filamentary structures formed by ion acceleration at the quasi-parallel bow shock. *Journal of Geophysical Research: Space Physics*, 119(4), 2593-2604. Retrieved from <https://agupubs.onlinelibrary.wiley.com/doi/abs/10.1002/2013JA019587> doi: 10.1002/2013JA019587
- Palmroth, M., Archer, M., Vainio, R., Hietala, H., Pfau-Kempf, Y., Hoilijoki, S., ... Eastwood, J. P. (2015). ULF foreshock under radial IMF: THEMIS observations and global kinetic simulation Vlasiator results compared. *Journal of Geophysical Research: Space Physics*, 120(10), 8782-8798. Retrieved from <https://agupubs.onlinelibrary.wiley.com/doi/abs/10.1002/2015JA021526> doi: 10.1002/2015JA021526
- Palmroth, M., Hietala, H., Plaschke, F., Archer, M., Karlsson, T., Blanco-Cano, X., ... others (2018). Magnetosheath jet properties and evolution as determined by a global hybrid-vlasov simulation. In *Annales geophysicae*.
- Pilipenko, V., Belakhovsky, V., Kozlovsky, A., Fedorov, E., & Kauristie, K. (2014). ULF wave modulation of the ionospheric parameters: Radar and magnetometer observations. *Journal of Atmospheric and Solar-Terrestrial Physics*, 108, 68-76.
- Pilipenko, V., Belakhovsky, V., Murr, D., Fedorov, E., & Engebretson, M. (2014). Modulation of total electron content by ULF Pc5 waves. *Journal of Geophysical Research: Space Physics*, 119(6), 4358-4369.
- Posch, J. L., Engebretson, M. J., Weatherwax, A. T., Detrick, D. L., Hughes, W. J., & MacLennan, C. G. (1999). Characteristics of broadband ULF magnetic pulsations at conjugate cusp latitude stations. *Journal of Geophysical Research: Space Physics*, 104(A1), 311-331. Retrieved from <https://agupubs.onlinelibrary.wiley.com/doi/abs/10.1029/98JA02722> doi: 10.1029/98JA02722

- 483 Pulkkinen, A., Bernabeu, E., Thomson, A., Viljanen, A., Pirjola, R., Boteler, D., ...
 484 others (2017). Geomagnetically induced currents: Science, engineering, and
 485 applications readiness. *Space Weather*, *15*(7), 828–856.
- 486 Pulkkinen, A., & Kataoka, R. (2006). S-transform view of geomagnetically in-
 487 duced currents during geomagnetic superstorms. *Geophysical Research Letters*,
 488 *33*(12). Retrieved from [https://agupubs.onlinelibrary.wiley.com/doi/](https://agupubs.onlinelibrary.wiley.com/doi/abs/10.1029/2006GL025822)
 489 [abs/10.1029/2006GL025822](https://agupubs.onlinelibrary.wiley.com/doi/abs/10.1029/2006GL025822) doi: 10.1029/2006GL025822
- 490 Rae, I. J., Donovan, E. F., Mann, I. R., Fenrich, F. R., Watt, C. E. J., Milling,
 491 D. K., ... Balogh, A. (2005). Evolution and characteristics of global
 492 Pc5 ULF waves during a high solar wind speed interval. *Journal of Geo-*
 493 *physical Research: Space Physics*, *110*(A12). Retrieved from [https://](https://agupubs.onlinelibrary.wiley.com/doi/abs/10.1029/2005JA011007)
 494 agupubs.onlinelibrary.wiley.com/doi/abs/10.1029/2005JA011007 doi:
 495 10.1029/2005JA011007
- 496 Rae, I. J., Watt, C., Fenrich, F., Mann, I., Ozeke, L., & Kale, A. (2008). Energy de-
 497 position in the ionosphere through a global field line resonance. *Annales Geo-*
 498 *physicae*, *25*(12), 2529–2539.
- 499 Russell, C. T., Luhmann, J. G., Odera, T. J., & Stuart, W. F. (1983). The rate of
 500 occurrence of dayside Pc 3,4 pulsations: The L-value dependence of the IMF
 501 cone angle effect. *Geophysical Research Letters*, *10*(8), 663–666. Retrieved
 502 from [https://agupubs.onlinelibrary.wiley.com/doi/abs/10.1029/](https://agupubs.onlinelibrary.wiley.com/doi/abs/10.1029/GL010i008p00663)
 503 [GL010i008p00663](https://agupubs.onlinelibrary.wiley.com/doi/abs/10.1029/GL010i008p00663) doi: 10.1029/GL010i008p00663
- 504 Shen, X.-C., Shi, Q., Wang, B., Zhang, H., Hudson, M. K., Nishimura, Y., ... others
 505 (2018). Dayside Magnetospheric and Ionospheric Responses to a Foreshock
 506 Transient on 25 June 2008: 1. FLR Observed by Satellite and Ground-Based
 507 Magnetometers. *Journal of Geophysical Research: Space Physics*, *123*(8),
 508 6335–6346.
- 509 Shi, X., Baker, J. B. H., Ruohoniemi, J. M., Hartinger, M. D., Murphy, K. R., Ro-
 510 driguez, J. V., ... Angelopoulos, V. (2018). Long-Lasting Poloidal ULF Waves
 511 Observed by Multiple Satellites and High-Latitude SuperDARN Radars. *Jour-*
 512 *nal of Geophysical Research: Space Physics*, *123*(10), 8422–8438. Retrieved
 513 from [https://agupubs.onlinelibrary.wiley.com/doi/abs/10.1029/](https://agupubs.onlinelibrary.wiley.com/doi/abs/10.1029/2018JA026003)
 514 [2018JA026003](https://agupubs.onlinelibrary.wiley.com/doi/abs/10.1029/2018JA026003) doi: 10.1029/2018JA026003
- 515 Sibeck, D. G. (1990). A model for the transient magnetospheric response to
 516 sudden solar wind dynamic pressure variations. *Journal of Geophysical*
 517 *Research: Space Physics*, *95*(A4), 3755–3771. Retrieved from [https://](https://agupubs.onlinelibrary.wiley.com/doi/abs/10.1029/JA095iA04p03755)
 518 agupubs.onlinelibrary.wiley.com/doi/abs/10.1029/JA095iA04p03755
 519 doi: 10.1029/JA095iA04p03755
- 520 Sibeck, D. G., Phan, T.-D., Lin, R., Lepping, R., & Szabo, A. (2002). Wind ob-
 521 servations of foreshock cavities: A case study. *Journal of Geophysical Research:*
 522 *Space Physics*, *107*(A10), SMP–4.
- 523 Takahashi, K., Lee, D.-H., Merkin, V. G., Lyon, J. G., & Hartinger, M. D. (2016).
 524 On the origin of the dawn-dusk asymmetry of toroidal Pc5 waves. *Jour-*
 525 *nal of Geophysical Research: Space Physics*, *121*(10), 9632–9650. Retrieved
 526 from [https://agupubs.onlinelibrary.wiley.com/doi/abs/10.1002/](https://agupubs.onlinelibrary.wiley.com/doi/abs/10.1002/2016JA023009)
 527 [2016JA023009](https://agupubs.onlinelibrary.wiley.com/doi/abs/10.1002/2016JA023009) doi: 10.1002/2016JA023009
- 528 Takahashi, K., McPherron, R. L., & Terasawa, T. (1984). Dependence of the
 529 spectrum of Pc 3-4 pulsations on the interplanetary magnetic field. *Jour-*
 530 *nal of Geophysical Research: Space Physics*, *89*(A5), 2770–2780. Retrieved
 531 from [https://agupubs.onlinelibrary.wiley.com/doi/abs/10.1029/](https://agupubs.onlinelibrary.wiley.com/doi/abs/10.1029/JA089iA05p02770)
 532 [JA089iA05p02770](https://agupubs.onlinelibrary.wiley.com/doi/abs/10.1029/JA089iA05p02770) doi: 10.1029/JA089iA05p02770
- 533 Wang, B., Nishimura, Y., Hietala, H., Shen, X.-C., Shi, Q., Zhang, H., ... others
 534 (2018). Dayside Magnetospheric and Ionospheric Responses to a Foreshock
 535 Transient on 25 June 2008: 2. 2-D Evolution Based on Dayside Auroral Imag-
 536 ing. *Journal of Geophysical Research: Space Physics*, *123*(8), 6347–6359.
- 537 Wright, A. N., Elsden, T., & Takahashi, K. (2018). Modeling the dawn/dusk asym-

- 538 metry of field line resonances. *Journal of Geophysical Research: Space Physics*,
539 123(8), 6443-6456. Retrieved from [https://agupubs.onlinelibrary.wiley](https://agupubs.onlinelibrary.wiley.com/doi/abs/10.1029/2018JA025638)
540 .com/doi/abs/10.1029/2018JA025638 doi: 10.1029/2018JA025638
- 541 Yagova, N. V., Pilipenko, V. A., Lanzerotti, L. J., Engebretson, M. J., Rodger,
542 A. S., Lepidi, S., & Papitashvili, V. O. (2004). Two-dimensional struc-
543 ture of long-period pulsations at polar latitudes in Antarctica. *Journal of*
544 *Geophysical Research: Space Physics*, 109(A3). Retrieved from [https://](https://agupubs.onlinelibrary.wiley.com/doi/abs/10.1029/2003JA010166)
545 agupubs.onlinelibrary.wiley.com/doi/abs/10.1029/2003JA010166 doi:
546 10.1029/2003JA010166
- 547 Yumoto, K., Saito, T., Akasofu, S.-I., Tsurutani, B. T., & Smith, E. J. (1985).
548 Propagation mechanism of daytime Pc 3-4 pulsations observed at syn-
549 chronous orbit and multiple ground-based stations. *Journal of Geophys-ical*
550 *Research: Space Physics*, 90(A7), 6439-6450. Retrieved from [https://](https://agupubs.onlinelibrary.wiley.com/doi/abs/10.1029/JA090iA07p06439)
551 agupubs.onlinelibrary.wiley.com/doi/abs/10.1029/JA090iA07p06439
552 doi: 10.1029/JA090iA07p06439
- 553 Zhang, H., Sibeck, D. G., Zong, Q.-G., Omid, N., Turner, D., & Clausen, L. (2013).
554 Spontaneous hot flow anomalies at quasi-parallel shocks: 1. observations. *Jour-*
555 *nal of Geophysical Research: Space Physics*, 118(6), 3357-3363.
- 556 Zhang, X. Y., Zong, Q.-G., Wang, Y. F., Zhang, H., Xie, L., Fu, S. Y., ... Pu, Z. Y.
557 (2010). ULF waves excited by negative/positive solar wind dynamic pressure
558 impulses at geosynchronous orbit. *Journal of Geophysical Research: Space*
559 *Physics*, 115(A10). Retrieved from [https://agupubs.onlinelibrary.wiley](https://agupubs.onlinelibrary.wiley.com/doi/abs/10.1029/2009JA015016)
560 .com/doi/abs/10.1029/2009JA015016 doi: 10.1029/2009JA015016
- 561 Zong, Q., Rankin, R., & Zhou, X. (2017). The interaction of ultra-low-frequency
562 Pc3-5 waves with charged particles in Earth's magnetosphere. *Reviews of Mod-*
563 *ern Plasma Physics*, 1(1), 10.